Radiology

Pulmonary Dysfunction after Pediatric COVID-19

Manuscript Type: Original Research

Rafael Heiss, MD[1*], Lina Tan[2*], Sandy Schmidt[1], Adrian P. Regensburger, MD[2,3], Franziska Ewert, MD[2,4], Dilbar Mammadova, MD[2,4], Adrian Buehler, MSc[2,3], Jens Vogel-Claussen, MD[5], Andreas Voskrebenzev, PhD[5], Manfred Rauh, PhD[2], Oliver Rompel, MD[1], Armin M. Nagel, MD[1], Simon Lévy, MD[1], Sebastian Bickelhaupt, MD[1], Matthias S. May, MD[1], Michael Uder, MD[1], Markus Metzler, MD[2], Regina Trollmann, MD[2,4], Joachim Woelfle, MD[2,4], Alexandra L. Wagner, MD[2,3,4**], Ferdinand Knieling, MD[2,3,4**#]

* R.H. and L.T. contributed equally to this work.
** A.L.W. and F.K. are co-senior authors.
[#] Corresponding author

[1] Institute of Radiology, University Hospital Erlangen, Friedrich-Alexander-Universität (FAU) Erlangen-Nürnberg, Germany

[2] Department of Pediatrics and Adolescent Medicine, University Hospital Erlangen, Friedrich-Alexander-Universität (FAU) Erlangen-Nürnberg, Germany

[3] Translational Experimental and Molecular Imaging Laboratory (PETI Lab), Department of Pediatrics and Adolescent Medicine, University Hospital Erlangen, Friedrich-Alexander-Universität (FAU) Erlangen-Nürnberg, Germany

[4] Center for Social Pediatrics, University Hospital Erlangen, Friedrich-Alexander-Universität (FAU) Erlangen-Nürnberg, Germany

[5] Institute for Diagnostic and Interventional Radiology, Hannover Medical School, Hannover, Germany.

Correspondence:
PD Dr. med. habil. Ferdinand Knieling
Departments of Pediatrics and Adolescent Medicine
University Hospital Erlangen
Friedrich-Alexander-Universität (FAU) Erlangen-Nürnberg
ferdinand.knieling@uk-erlangen.de

Funding

Junior project (J089) and Clinician Scientist Program (CSP) from the Interdisciplinary Center for Clinical Research (IZKF) at the Friedrich-Alexander-Universität (FAU) Erlangen-Nürnberg

for A.P.R. This work received funding from the Bayerisches Staatsministerium für Wissenschaft und Kunst. The funding bodies had no role in the study design, collection, analysis, interpretation of data, writing of the report, or decision to submit the article for publication.

Data sharing statement

Data generated or analyzed during the study are available from the corresponding author by request.

Summary

Low-field MRI showed persistent pulmonary dysfunction in both children and adolescents recovered from COVID-19 and with long COVID.

Key Results

- In a prospective clinical trial, 54 children and adolescents with previous SARS-CoV-2 infection (29 recovered, 25 with long COVID) were compared with nine healthy controls using low-field MRI.

- Both ventilated and perfused lung parenchyma (V/Q match) was 81 ± 6% in healthy controls, 62 ± 19% (*P*=.006) in the recovered group, and 60 ± 20% (*P*=.003) in the long COVID group.

- V/Q match was lower in post COVID participants with infection less than 180 days (63 ± 20%, *P*=.03), 180 to 360 days (63 ± 18%, *P*=0.03) and 360 days (41 ± 12%, *P*<.001) compared to never-infected healthy controls (81 ± 6.1%).

Abbreviations

VDP=ventilation defect percentage, QDP=perfusion defect percentage, V/Q=ventilation-perfusion

Abstract

Background

Long COVID occurs in lower frequency in children and adolescents than in adults. Morphologic and free-breathing phase-resolved functional low-field MRI may identify persistent pulmonary manifestations after SARS-CoV-2 infection.

Purpose

To characterize both morphologic and functional changes of lung parenchyma on low-field MRI in children and adolescents with post COVID-19 compared with healthy controls.

Materials and Methods

Between August and December 2021, a cross-sectional, prospective clinical trial using low-field MRI was performed in children and adolescents from a single academic medical center. The primary outcome was the frequency of morphologic changes on MRI. Secondary outcomes included MRI-derived functional proton ventilation and perfusion parameters. Clinical symptoms, the duration from positive RT-PCR test and serological parameters were compared with imaging results. Nonparametric tests for pairwise and corrected tests for groupwise comparisons were applied to assess differences in healthy controls, recovered participants and with long COVID.

Results

A total of 54 participants post COVID-19 infection (mean age, 11 years ±3 [SD], 56 males) and 9 healthy controls (mean age, 10 years ±3 [SD], 70 males) were included: 29 (54%) in the COVID-19 group had recovered from infection and 25 (46%) were classified as having long COVID on the day of enrollment. Morphologic abnormality was identified in one recovered participant. Both ventilated and perfused lung parenchyma (V/Q match) was reduced from 81±6.1% in healthy controls to 62±19% (P =.006) in the recovered group and 60±20% (P=.003) in the long COVID group. V/Q match was lower in post COVID patients with infection less than 180 days (63±20%, P=.03), 180 to 360 days (63±18%, P=0.03) and 360 days ago (41±12%, P<.001) as compared with the never-infected healthy controls (81±6.1%).

Conclusion

Low-field MRI showed persistent pulmonary dysfunction in both children and adolescents recovered from COVID-19 and with long COVID.

ClinicalTrials.gov: NCT04990531

Introduction

SARS-CoV-2 has emerged as a global pandemic causing more than 280 million documented infections and 5.4 million deaths until the end of 2021.[1] In comparison with adults, COVID-19 in children and adolescents has a milder course, with recovery within a few weeks.[2] There is heterogeneity in the definition and inconsistency in reporting persistent symptoms ranging from near 0 to 66% for several months after infection.[3-8] These findings are further complicated by the fact, that there are more objective findings of post-acute sequelae and symptoms in younger patients.[2,6]

While there is an increasing understanding of the multi-organ damage of COVID-19 beyond the acute phase of infection[9], the nature, frequency, and definition of post-acute sequelae in children and adolescents still remains unknown, with a discrepancy in the clinical appearance and objective findings.[10] While a number of pediatric studies have lately prioritized research in mental health issues during the COVID-19 pandemic[11,12], other studies have raised concerns about ongoing disease manifestations, such as increased thrombotic state, microangiopathy, and inflammation.[13,14]

As the lung is a primary target of the SARS-CoV-2 virus,[15] CT has aided in the diagnosis of pulmonary manifestation of COVID-19 in adults.[16] Even three months after infection, angiographic imaging of pulmonary microcirculation has revealed widespread microangiopathy in over 65% of patients.[17] Such techniques using invasive procedures or ionization radiation are not feasible in children. They also seem to have limited diagnostic value as lung parenchymal changes due to COVID-19 are less obvious and pronounced in children.[18,19] Therefore, there is an unmet clinical need to characterize pulmonary manifestations more precisely in children and adolescents after SARS-CoV-2 infection.

We used low-field MRI for imaging the pediatric lung. At low field strength, this technique has improved the imaging quality of near air-tissue interfaces, without the need for ionizing radiation.[20,21] The aim of the study was to characterize the morphologic and functional changes of lung parenchyma on low-field MRI in children and adolescents with previous RT-PCR-positive SARS-CoV-2 infection compared with healthy controls.

Materials and Methods

Trial design

This prospective study was approved by the local ethics committee (No 21-206-B). All parents/guardians and participants (if appropriate) gave written informed consent to participate in the study.

The subject number calculation for the group comparison of two independent samples was derived from the preliminary data. It was based on the expected perfusion deficit. In the healthy group, the value was expected to be 1, whereas in the diseased group the value was 16. With a common (weighted) standard deviation of 11.5, the group size was determined to be 10 (per group). With a sensitivity of 90%, specificity of 85%, precision of ±0.15, estimated prevalence of 0.3, confidence level of 95% and a 10% rate of dropout, the power calculation yielded 58 subjects (including dropouts).

Between August 2021 and December 2021, we performed a cross-sectional, investigator-initiated trial to investigate lung parenchymal changes in children and adolescents after SARS-CoV-2 infection (ClinicalTrials.gov: NCT04990531) at a single academic medical center. We enrolled consecutive patients with COVID-19 from a nationwide search. After assessment for clinical parameters, a blood sample was drawn and all participants with COVID-19 and healthy controls underwent low-field MRI. Clinical features during and after infection, the time period from positive RT-PCR test and laboratory parameters were compared with imaging results. Details are provided in the protocol and the statistical analysis plan.

The coordinating clinical investigators were responsible for data collection and site monitoring. The first authors and corresponding author had constant access to the data and performed the statistical analysis as well as the creation of the first draft of the manuscript independent from commercial support.

Participants

In the COVID-19 group, inclusion criteria consisted of a required age between 5 and below 18 years of age. Eligible patients were required to have a documented positive RT-PCR-test for SARS-CoV-2, regardless of the interval between positive testing and inclusion in the study. Exclusion criteria consisted of acute SARS-CoV-2 infection and a need for isolation/quarantine

measures, pregnancy, any critical medical condition, the refusal of MRI and any contraindications to MRI (e.g., electrical implants such as pacemakers or perfusion pumps etc.). In the healthy control group, inclusion criteria consisted of a required age between 5 and below 18 years of age. Healthy controls were excluded when there was a previous positive SARS-CoV-2 infection confirmed by RT-PCR or rapid antigen test, any clinical or other suspicion of pulmonary disease, current respiratory infection/symptomatology, pain resulting in respiratory limitation, acute SARS-CoV-2 infection and need for isolation, need for quarantine, pregnancy, critical condition, the refusal of MRI or general contraindications to MRI examinations (e.g., electrical implants such as pacemakers or perfusion pumps etc.). In addition, patients were excluded if they were found positive for SARS-CoV-2 antibodies in their respective blood sample.

Definition of long COVID

The definition for long COVID was based on the persistence of symptoms for a minimum of 12 weeks and either one of the four following criteria:[22,23] 1) Symptoms that persisted from the acute COVID-19 phase or its treatment, 2) Symptoms that resulted in a new health limitation, 3) New symptoms that occurred after the end of the acute phase but were understood to be a consequence of COVID-19 disease, 4) Worsening of a pre-existing underlying medical condition. This guideline reflects the current WHO definition of long COVID.[24]

Outcome measures

The primary outcome was the determination of the frequency of morphological changes of lung parenchyma by low-field proton MRI. Secondary outcomes included functional lung changes comprising ventilation defects (ventilation defect percentage; whole-lung VDP), perfusion defects (perfusion defect percentage; whole-lung QDP), the match (ventilation/perfusion match; V/Q match) and defect of both (ventilation/perfusion defect; whole-lung V/Q defect), laboratory assessments and reported clinical symptoms.

Clinical data and blood samples

Participants in the COVID-19 group were assessed for medical history, including symptoms during and after COVID-19 infection. Blood pressure and heart rate were measured from each individual. A blood sample was collected to assess blood count, interleukin 6 (IL-6), C-reactive protein (Carp) and antibodies against SARS-CoV-2 (spike protein and nucleocapsid antibodies,

electrochemiluminescence immunoassay (ECLIA), Anti-SARS-Cov-2 S [Elecsys], and Anti-SARS-CoV2 [Roche]); for details see Methods section in Appendix E1).

MRI protocol

All participants underwent morphological and functional low-field MRI (low-field MRI, 0,55 Tesla MAGNETOM Free.Max, Siemens Healthineers) for visualization of morphological features, ventilation and perfusion of the lung.[25-29] For all investigations a standard body coil was used for free-breathing lung imaging. The final parameters were: one two-dimensional central coronal slice positioned at the middle of the lung hila, thickness=15mm, in-plane resolution=1.7x1.7mm^2, matrix=128x128 (interpolated to 256x256), bandwidth=1149Hz/pixel, flip angle=80°, TR/TE=292.8/1.6ms, parallel imaging acceleration factor =2, no partial Fourier, 250 time points, temporal resolution=300ms, duration=1min15s. For all MRI data and analyses, the evaluating radiologist (R. H.) was blinded to clinical features.

Morphologic lung imaging

For morphological lung assessment, a coronal and transversal Turbo-Spin-Echo (TSE) sequence with BLADE (periodically rotated overlapping parallel lines with enhanced reconstruction) readout and respiration-gating were acquired. The coronal image was acquired with a STIR preparation (Short-Inversion Time Inversion Recovery), T2-weighting (TE/TR=74/2500ms), 1.5×1.5mm^2 in-plane resolution, 272x272 matrix, 6mm thickness. The transversal image was proton density-weighted (TE/TR=33/2000ms) with 1.3×1.3mm^2 in-plane resolution, 304x304 matrix, 6mm thickness.

Functional lung assessment

For free-breathing phase-resolved functional lung (PREFUL) low-field MRI, the following parameters were calculated voxel-wise by using a dedicated software (MR Lung v2.0, Siemens Healthcare) after automatic registration to a mid-expiration position and lung parenchyma segmentation.[26]

Normalized perfusion (Q, %) with respect to a full-blood signal region, determined as the highest perfusion signal region in-between the lungs and expected to reflect the aorta or other available large vessel [27]; Regional ventilation (V, %) calculated as: $\frac{S_{mid}}{S_{insp}} - \frac{S_{mid}}{S_{exp}}$ with S the signal value at end-inspiration ($insp$), end-expiration (exp) and middle position (mid); [30] Flow-Volume Loop correlation (FVL): correlation of the Flow-Volume Loop (deduced from the V reconstructed cycle) with respect to a healthy region (largest connected region within the 80th

and 90th V percentiles).[31] Based on those maps, the percentage of defect areas (QDP, VDP) were calculated based on thresholds optimized on a large sample (of 155 healthy volunteers and 95 patients with various lung diseases scanned at 1.5T with a Fast Low-Angle Shot sequence (perfusion: 2%, FV: 40% of the 90th percentile, FVL: 0.9). The percentage of concurrent defect areas of perfusion and ventilation metrics (V/Q defect, V/Q defect, $_{FVL}$) and perfusion defects exclusive to ventilation defects ($QDP_{Exclusive}$) were derived, and vice versa ($VDP_{FVL,Exclusive}$, $VDP_{Exclusive}$). In addition, areas without defects on both perfusion and ventilation maps (V/Q match, V/Q match, $_{FVL}$) were calculated. An overview and explanation of all parameters used is given in **Table 1**. *PREFUL MRI ventilation and perfusion measures were recently validated using V/Q SPECT, dynamic contrast-enhanced MRI, as well as ^{19}F and ^{129}Xe inhaled gas MRI.*[27,32]

Statistical analyses

Continuous variables are given as mean value with standard deviation, categorical variables as numbers with percentages. The occurrence of MRI changes is given as a percentage of the population. A nonparametric Mann-Whitney test was used for pairwise comparisons. A non-parametric Kruskal-Wallis test with corrected Dunn's test for post-hoc comparisons between groups was used to assess differences in healthy controls, participants who recovered from COVID-19, and participants with long COVID. Adjusted p values are reported. Prism 9, version 9.3.1 (GraphPad Software) was used for all statistical analyses. A P value of less than .05 was considered to indicate statistical significance in all analyses.

Results

Participant Characteristics

A total of 17 healthy controls and 91 pediatric patients after RT-PCR-positive SARS-CoV-2 infection were screened. 7 healthy controls and 33 patients with post-acute COVID-19 were excluded prior to participation. 1 healthy control had a pulmonary nodule of unknown dignity on morphologic MRI and was therefore excluded. 4 patients with post-acute COVID-19 were not able to complete low-field MRI scanning and were therefore excluded. Overall, 54 participants with post-acute COVID-19 and 9 controls completed clinical, laboratory, and low-field MRI assessments (**Figure 1**).

The characteristics of the participants were similar in both groups (**Table 2**). The mean age of participants with post-acute COVID-19 was 12±3 years (control: 10±3 years), mean weight was 48±18kg (40±15kg), mean height was 156±17 (144±11cm) and 44% (30%) were female. Of the 54 participants with RT-PCR-positive SARS-CoV-2 infection, 29 (54%) had recovered from infection while 25 participants (46%) were classified as having long COVID. 5 participants reported headache (9%), 15 dyspnea (28%), 1 pneumonia (2%), 4 anosmia (7%), 1 ageusia (2%), 4 fatigue (7%), 6 impaired attention (11%), 1 limb pain (2%) and 16 shortness of breath (30%) (**Table E1**). Pre-existing conditions were found in 22% of the healthy volunteers, 5% of the recovered and 10% of the long COVID-19 patients (for a detailed overview see **Table E1**). Detailed acute and post-acute COVID-19 symptoms can be found in **Table E2**. 4 participants with RT-PCR-positive SARS-CoV2 infection did not show any symptoms during acute infection. None of the COVID-19 group required hospital admission during the primary infection period. The median interval between positive SARS-CoV-2 RT-PCR test and study participation were 222±134 days. There were no missing primary and/or secondary outcome data.

Primary outcome

Of the 54 participants in the post-acute COVID-19 group and 9 healthy controls scanned with low-field MRI, only 1 participant in the recovered group showed any morphological changes (linear atelectasis) (**Figure E1**).

Secondary outcomes

When compared with healthy controls, larger ventilation defects (VDP; 13±3.6% vs. 23±9.0%, $P<.001$), perfusion defects (QDP; 6.5±5.0% vs. 20±19%, $P=.05$) and combined defects (V/Q mismatch; 0.5±0.8 vs. 4.6±5.7, $P=.001$) were found in diseased participants using functional

low-field MRI. V/Q match was lower in the post-COVID group (61±19%, *P*<.001) when compared to healthy controls (81±6.1%) (**Figure E2**).

When separating the COVID-19 group by clinical characteristics, the overall VDP was lower in healthy controls (13±3.6%) than in the recovered (22±8.1%, *P*=.01) or the long COVID group (25±10%, *P*=.002). Similarly, QDP was higher in the recovered (19±19%, *P*=0.35) and in the long COVID group (22±19%, *P*=.10) as compared to healthy controls (6.5±5.0%). Combined V/Q defects were lower in healthy controls with 0.5±0.8% compared to 3.9±4.7% (*P*=.04) in the recovered and 5.4±6.6% (*P*=.002) in the long COVID group. Similarly, V/Q match was higher in healthy controls with 81±6.1% compared to 62±19% (*P*=.006) in the recovered and 60±20 (*P*=.003) in the long COVID group (**Table 3, Figure E3, Table E3** in the Appendix E1 for further parameters). Representative functional low-field MRI images are shown in **Figure 2;** the corresponding morphologic images are shown in **Figure E4**. For a complete imaging list displaying combined ventilation/perfusion defects see **Figures E5-7** in the Appendix E1.

When separating participants according to duration from infection, an increase in ventilation, perfusion, and combined defects were found (**Figure 3A-C**). In turn, V/Q match was reduced in post COVID patients with infection less than 180 days ago (63±20%, P=.03), to 63±17.5% in patients infected 180 to 360 days ago (P=0.03) and to 41±12% in patients infected 360 days ago (P<.001) as compared to never-infected healthy controls (81±6.1%) (**Figure 3D**).

Laboratory assessments

From the 54 participants with post-acute COVID-19, 4 showed negative spike protein and nucleocapsid antibody level at time of presentation (time range to RT-PCR-proven infection 186-416 days). 2 participants with post-acute COVID-19 had reactive spike protein antibodies without reactive nucleocapsid antibodies (time range to RT-PCR-proven infection 40-339 days). All 9 healthy controls were confirmed with negative spike protein and nucleocapsid antibody levels.

Inflammation parameters including CrP, IL-6 and blood counts were not suggestive of a current infection at the day of study for any participant.

Discussion

The purpose of the study was to characterize both morphologic and functional changes of lung parenchyma on low-field MRI in children and adolescents with post COVID-19 compared with healthy controls. A total of 54 post COVID children and adolescents (29 recovered, 25 with long COVID) and 9 healthy controls were included. Only one participant showed any morphologic abnormality (linear atelectasis). Using functional parameters, we found a reduction of V/Q match from 81.2±6.1% in healthy controls to 62.0±18.7% (*P*=.006) in the recovered group and 59.9±19.8% (*P*=.003) in the long COVID group. Furthermore, V/Q match was lower in COVID patients with infection less than 180 days (63.5±20.1%, *P*=.03), 180 to 360 days (63.15±17.5%, *P*=0.03) and 360 days ago (41.5±11.9%, *P*<.001) as compared to never-infected healthy controls (81.2±6.1%).

Similar imaging approaches to the one used in our study have already proven to be able to visualize pathologic changes in pulmonary hypertension, cystic fibrosis, and chronic obstructive pulmonary disease.[27-29] Specifically for COVID-19, our findings correspond to observations in adults, where vascular[17] or structural abnormalities[33] persist in previously hospitalized adults. Another technique using inhaled gas contrasts agents (Hyperpolarized ^{129}Xe MRI) to assess lung function has already been successfully applied in adults with post COVID-19. These studies had normal findings on CT, however they did show a limitation pulmonary capillary gas diffusion.[34,35] In a recent study on 34 post COVID adult patients, of whom 22 had never been hospitalized, and six controls, a correlation of ^{129}Xe MRI parameters and CT pulmonary vascular abnormalities was described.[36] Interestingly, Trinkman et al. were also able to demonstrate that one half of mostly younger adult study subjects have persistent symptoms and reduced lung function for more than two months after infection.[37] These results may partly correspond to the high frequency of abnormal imaging findings in our population, wherein 28% of post COVID-19 participants still reported dyspnea and 30% shortness of breath.

The low-field MRI (0.55T) used in this study has advantages for the morphological imaging of lung parenchyma when compared to 1.5T and 3T systems.[20] In contrast to studies that are mostly based on surveys or self-reported outcomes, which suggest less severe COVID-19 infections and sequelae in younger patients, our study demonstrates widespread functional lung alterations are indeed present in children and adolescents. This expands the understanding of pediatric post-acute COVID-19 disease, particularly given the increased incidence of SARS-CoV-2 infection.[1] A better estimate on the prevalence on pediatric post COVID lung disease

is further complicated by the inconsistent, largely symptom-based definitions of long COVID disease[9] - and its limited applicability to children.

The pathophysiology of acute and post-acute pathology of COVID-19 partly originates from direct endothelial damage, local inflammation, and prothrombotic milieu.[15,38,39] A proposed mechanism is the ACE2-mediated entry of SARS-CoV-2, which allows the virus to directly invade endothelial cells.[15,40] This may explain manifestations such as pulmonary microangiopathy and widespread capillary microthrombi seen in autopsies from patients who died from COVID-19[15] and fibrotic-like consolidations found in CT.[33] Previously described[14] persistent signs of inflammatory processes could not be confirmed in our study. As children develop a robust, cross-reactive, and sustained immune response after SARS-CoV-2 infection[41], the observed pulmonary dysfunction in our study is an unexpected finding.

Our study had several limitations. First, we did not compare our measurements to another reference standard, such as ventilation-perfusion scintigraphy, spirometry, or body plethysmography. However, most of these modalities either use ionization radiation, are invasive, or require active cooperation. Second, the functional low-field MRI in our study used free-breathing all intervals, which was feasible in 93% of the pediatric post-acute COVID-19 group starting from 5 years of age. Third, our study lacked longitudinal data. Fourth, we had a low number of healthy controls. Finally, a selection bias does exist, as families with children with acute or post-acute symptomatic COVID-19 and higher disease burden might have been more likely to participate in our study.

In summary, we report persistent pulmonary dysfunction as visualized on low-field MRI in both children and adolescents recovered from COVID-19 and with long COVID. The further course and outcome of the observed changes currently remains unclear. Our results warrant further surveillance of persistent pulmonary damage in pediatrics and adolescents after SARS-CoV-2 infection. Given the already existing diagnostic value of lung MRI[42] and the translatability of the technology, these imaging approaches can be rapidly adopted to clinical routine care.

Acknowledgments

We thank the Imaging Science Institute Erlangen for providing us with measurement time and technical support. Many thanks to Natalie Wenisch, Kristin Pribylla und Annika Maischak for technical assistance during MR imaging and the staff of the social pediatrics center at the University Hospital Erlangen during patient recruitment.

The present work was performed in (partial) fulfillment of the requirements for obtaining the degree „Dr. med." for L.T. and in (partial) fulfillment of the requirements for obtaining the degree „Dr. rer. biol. hum." for A.P.R.

Competing interests

R.H., M.U. and M.M. are part of the speakers bureau of the Siemens Healthcare GmbH. The authors have no further affiliation with any organization with a direct or indirect financial interest in the subject matter discussed in the manuscript. F.K. received speaker honorary from Siemens Healthcare GmbH. All other authors declare no conflict of interest.

References

1 *WHO Health Emergency Dashboard*, <https://covid19.who.int>

2 Say, D. *et al.* Post-acute COVID-19 outcomes in children with mild and asymptomatic disease. *Lancet Child Adolesc Health* **5**, e22-e23, doi:10.1016/S2352-4642(21)00124-3 (2021).

3 Behnood, S. A. *et al.* Persistent symptoms following SARS-CoV-2 infection amongst children and young people: A meta-analysis of controlled and uncontrolled studies. *J Infect* **84**, 158-170, doi:10.1016/j.jinf.2021.11.011 (2022).

4 Sterky, E. *et al.* Persistent symptoms in Swedish children after hospitalisation due to COVID-19. *Acta Paediatr* **110**, 2578-2580, doi:10.1111/apa.15999 (2021).

5 Radtke, T., Ulyte, A., Puhan, M. A. & Kriemler, S. Long-term Symptoms After SARS-CoV-2 Infection in Children and Adolescents. *JAMA*, doi:10.1001/jama.2021.11880 (2021).

6 Buonsenso, D. *et al.* Preliminary evidence on long COVID in children. *Acta Paediatr* **110**, 2208-2211, doi:10.1111/apa.15870 (2021).

7 Osmanov, I. M. *et al.* Risk factors for post-COVID-19 condition in previously hospitalised children using the ISARIC Global follow-up protocol: a prospective cohort study. *Eur Respir J* **59**, doi:10.1183/13993003.01341-2021 (2022).

8 Kikkenborg Berg, S. *et al.* Long COVID symptoms in SARS-CoV-2-positive children aged 0-14 years and matched controls in Denmark (LongCOVIDKidsDK): a national, cross-sectional study. *Lancet Child Adolesc Health*, doi:10.1016/S2352-4642(22)00154-7 (2022).

9 Nalbandian, A. *et al.* Post-acute COVID-19 syndrome. *Nat Med* **27**, 601-615, doi:10.1038/s41591-021-01283-z (2021).

10 Zimmermann, P., Pittet, L. F. & Curtis, N. How Common is Long COVID in Children and Adolescents? *Pediatr Infect Dis J* **40**, e482-e487, doi:10.1097/INF.0000000000003328 (2021).

12 Zavala, M., Ireland, G., Amin-Chowdhury, Z., Ramsay, M. E. & Ladhani, S. N. Acute and persistent symptoms in children with PCR-confirmed SARS-CoV-2 infection compared to test-negative children in England: active, prospective, national surveillance. *Clin Infect Dis*, doi:10.1093/cid/ciab991 (2021).

13 Fogarty, H. *et al.* Persistent endotheliopathy in the pathogenesis of long COVID syndrome. *J Thromb Haemost* **19**, 2546-2553, doi:10.1111/jth.15490 (2021).

14 Buonsenso, D. *et al.* Evidence of lung perfusion defects and ongoing inflammation in an adolescent with post-acute sequelae of SARS-CoV-2 infection. *Lancet Child Adolesc Health* **5**, 677-680, doi:10.1016/S2352-4642(21)00196-6 (2021).

15 Ackermann, M. *et al.* Pulmonary Vascular Endothelialitis, Thrombosis, and Angiogenesis in Covid-19. *N Engl J Med* **383**, 120-128, doi:10.1056/NEJMoa2015432 (2020).

16 Ai, T. *et al.* Correlation of Chest CT and RT-PCR Testing for Coronavirus Disease 2019 (COVID-19) in China: A Report of 1014 Cases. *Radiology* **296**, E32-E40, doi:10.1148/radiol.2020200642 (2020).

17 Remy-Jardin, M. *et al.* Assessment of pulmonary arterial circulation 3 months after hospitalization for SARS-CoV-2 pneumonia: Dual-energy CT (DECT) angiographic study in 55 patients. *EClinicalMedicine* **34**, 100778, doi:10.1016/j.eclinm.2021.100778 (2021).

18 Shelmerdine, S. C., Lovrenski, J., Caro-Dominguez, P., Toso, S. & Collaborators of the European Society of Paediatric Radiology Cardiothoracic Imaging, T. Coronavirus disease 2019 (COVID-19) in children: a systematic review of imaging findings. *Pediatr Radiol* **50**, 1217-1230, doi:10.1007/s00247-020-04726-w (2020).

19 Steinberger, S. *et al.* CT Features of Coronavirus Disease (COVID-19) in 30 Pediatric Patients. *AJR Am J Roentgenol* **215**, 1303-1311, doi:10.2214/AJR.20.23145 (2020).
20 Campbell-Washburn, A. E. *et al.* Opportunities in Interventional and Diagnostic Imaging by Using High-Performance Low-Field-Strength MRI. *Radiology* **293**, 384-393, doi:10.1148/radiol.2019190452 (2019).
21 Rashid, S. *et al.* Cardiac balanced steady-state free precession MRI at 0.35 T: a comparison study with 1.5 T. *Quant Imaging Med Surg* **8**, 627-636, doi:10.21037/qims.2018.08.09 (2018).
22 Koczulla, A. *et al.* S1-Leitlinie Post-COVID/Long-COVID. *AWMF online* (2021).
23 Ceravolo, M. G. *et al.* Rehabilitation and COVID-19: the Cochrane Rehabilitation 2020 rapid living systematic review. *Eur J Phys Rehabil Med* **56**, 642-651, doi:10.23736/S1973-9087.20.06501-6 (2020).
25 Heiss, R. *et al.* High-performance low field MRI enables visualization of persistent pulmonary damage after COVID-19. *Magnetic resonance imaging* **76**, 49-51, doi:10.1016/j.mri.2020.11.004 (2021).
26 Voskrebenzev, A. *et al.* Feasibility of quantitative regional ventilation and perfusion mapping with phase-resolved functional lung (PREFUL) MRI in healthy volunteers and COPD, CTEPH, and CF patients. *Magn Reson Med* **79**, 2306-2314, doi:10.1002/mrm.26893 (2018).
27 Behrendt, L. *et al.* Validation of Automated Perfusion-Weighted Phase-Resolved Functional Lung (PREFUL)-MRI in Patients With Pulmonary Diseases. *J Magn Reson Imaging* **52**, 103-114, doi:10.1002/jmri.27027 (2020).
28 Glandorf, J. *et al.* Comparison of phase-resolved functional lung (PREFUL) MRI derived perfusion and ventilation parameters at 1.5T and 3T in healthy volunteers. *PloS one* **15**, e0244638, doi:10.1371/journal.pone.0244638 (2020).
29 Pohler, G. H. *et al.* Repeatability of Phase-Resolved Functional Lung (PREFUL)-MRI Ventilation and Perfusion Parameters in Healthy Subjects and COPD Patients. *J Magn Reson Imaging* **53**, 915-927, doi:10.1002/jmri.27385 (2021).
30 Klimes, F. *et al.* Free-breathing quantification of regional ventilation derived by phase-resolved functional lung (PREFUL) MRI. *NMR Biomed* **32**, e4088, doi:10.1002/nbm.4088 (2019).
31 Moher Alsady, T. *et al.* MRI-derived regional flow-volume loop parameters detect early-stage chronic lung allograft dysfunction. *J Magn Reson Imaging* **50**, 1873-1882, doi:10.1002/jmri.26799 (2019).
32 Kaireit, T. F. *et al.* Flow Volume Loop and Regional Ventilation Assessment Using Phase-Resolved Functional Lung (PREFUL) MRI: Comparison With (129) Xenon Ventilation MRI and Lung Function Testing. *J Magn Reson Imaging* **53**, 1092-1105, doi:10.1002/jmri.27452 (2021).
33 Han, X. *et al.* Six-month Follow-up Chest CT Findings after Severe COVID-19 Pneumonia. *Radiology* **299**, E177-E186, doi:10.1148/radiol.2021203153 (2021).
34 Li, H. *et al.* Damaged lung gas exchange function of discharged COVID-19 patients detected by hyperpolarized (129)Xe MRI. *Sci Adv* **7**, doi:10.1126/sciadv.abc8180 (2021).
35 Grist, J. T. *et al.* Hyperpolarized (129)Xe MRI Abnormalities in Dyspneic Patients 3 Months after COVID-19 Pneumonia: Preliminary Results. *Radiology* **301**, E353-E360, doi:10.1148/radiol.2021210033 (2021).
36 Matheson, A. M. *et al.* Persistent (129)Xe MRI Pulmonary and CT Vascular Abnormalities in Symptomatic Individuals with Post-Acute COVID-19 Syndrome. *Radiology*, 220492, doi:10.1148/radiol.220492 (2022).

37 Trinkmann, F. *et al.* Residual symptoms and lower lung function in patients recovering from SARS-CoV-2 infection. *Eur Respir J* **57**, doi:10.1183/13993003.03002-2020 (2021).
38 Teuwen, L. A., Geldhof, V., Pasut, A. & Carmeliet, P. COVID-19: the vasculature unleashed. *Nat Rev Immunol* **20**, 389-391, doi:10.1038/s41577-020-0343-0 (2020).
39 Varga, Z. *et al.* Endothelial cell infection and endotheliitis in COVID-19. *Lancet* **395**, 1417-1418, doi:10.1016/S0140-6736(20)30937-5 (2020).
40 McFadyen, J. D., Stevens, H. & Peter, K. The Emerging Threat of (Micro)Thrombosis in COVID-19 and Its Therapeutic Implications. *Circ Res* **127**, 571-587, doi:10.1161/CIRCRESAHA.120.317447 (2020).
41 Dowell, A. C. *et al.* Children develop robust and sustained cross-reactive spike-specific immune responses to SARS-CoV-2 infection. *Nat Immunol* **23**, 40-49, doi:10.1038/s41590-021-01089-8 (2022).
42 Hirsch, F. W. *et al.* The current status and further prospects for lung magnetic resonance imaging in pediatric radiology. *Pediatr Radiol* **50**, 734-749, doi:10.1007/s00247-019-04594-z (2020).

Table 1: **Functional Low-Field MRI Parameters**

Parameter	**Explanation**
FVL	Flow volume loop
Mean FVL Correlation	Ventilation derived by cross-correlation
V	Ventilation
Q	Perfusion
VDP	Ventilation defect percentage
QDP	Perfusion defected percentage
V/Q match	Ventilation/perfusion match
V/Q defect	Combined ventilation/perfusion defect
VDP_{FVL}	Ventilation defect percentage, based on flow-volume loop correlation metric
$V/Q\ defect_{, FVL}$	VQ defect based on Q and FVL
$V/Q\ match_{, FVL}$	VQ non-defect based on Q and FVL
Exclusive	Only singular affected parenchyma without corresponding other defects
$VDP_{FVL,Exclusive}$	Exclusive ventilation defect percentage, no concurrent Q defect, based on FVL correlation metric
$VDP_{Exclusive}$	Exclusive ventilation defect percentage, no concurrent Q defect, based on regional ventilation
$QDP_{Exclusive}$	Exclusive perfusion defect percentage, no concurrent V defect, based on normalized perfusion

Table 2: Demographic and Clinical Characteristics of the Study Participants

Characteristic	Healthy control (N=9)	Post COVID-19 (N=54)	
		Recovered (N=29)	Long COVID (N=25)
Age – yr†	10±3	11±3	12±3
Age group – no. (%)			
5-8 yr	3 (33)	7 (24)	3 (12)
8-12 yr	4 (44)	14 (48)	10 (40)
12-18 yr	2 (22)	8 (28)	12 (48)
Weight – kg	39.7±15.3	43.0±16.4	52.9±18.7
Height – cm	143.9±11.3	152.8±17.0	159.2±18.4
Sex – no. (%)			
Female	2 (22)	13 (45)	11 (44)
Male	7 (78)	16 (55)	14 (56)
Race or ethnic group – no. (%)			
Mixed, other	2 (22)	1 (2)	1
White	7 (78)	53 (98)	24
Elapsed time from positive RT-PCR – days	n/a	162±137	292±90
Vaccination prior to infection – no. (%)	n/a	1 (3)	0 (0)
Vaccination prior to inclusion – no. (%)	0 (0%)	7 (24)	11 (44)
Mild illness	n/a	29 (100)	25 (100)
Hospitalization after SARS-CoV-2 infection	n/a	0 (0)	0 (0)
Vital parameters			
Systolic blood pressure - mmHg	114±12	116±15	114±10
Diastolic blood pressure - mmHg	64±5	68±10	67±9
Heart rate – bpm	84±11	87±14	84±16
Laboratory assessments			
Hemoglobin – g/dl	13.3±0.8	13.2±1.1	13.8±1.3
Thrombocytes – $*10^3/\mu l$	309±61	295±69	278±52
Leukocytes – $*10^3/\mu l$	6.6±1.5	6.6±1.6	6.8±1.6
Interleukin 6 – ng/l	0.7±1.5	0.2±1.0	0.1±0.4
C-reactive protein – mg/l	0.5±0.5	0.5±0.8	0.6±0.9
SARS-CoV-2 serostatus			
Spike protein antibody — U/ml‡¶	0±0	3552±8164	8614±18178
Seropositive participants– No. (%)	0 (0)	28 (97)	22 (88)
Nucleocapsid antibody — U/ml‡¶	0±0	64±72	46±70
Seropositive participants– No. (%)	0 (0)	28 (97)	22 (88)

Note—Data in parentheses are percentages. Plus–minus values are means ±SD.

COVID-19 group, one participant had an African-German background.

† Age reflects the age at the date of signed informed consent.

‡ Serostatus at baseline was measured by Anti-SARS-Cov-2 S (Elecsys) and Anti-SARS-CoV2 (Roche).

Table 3: Quantitative Measurements of Free Breathing Phase-resolved Functional Lung MRI*

Parameter	Healthy control (N=9)	Recovered (N=29)	P Value †	Long COVID (N=25)	P Value †
Mean Perfusion - %	6.5±1.6	5.2±2.3	.22	5.0±2.3	.07
Mean Ventilation - %	14±3.4	14±3.9	>.99	16±6.5	>.99
Ventilation defect percentage (whole lung VDP) - %	13±3.6	22±8.1	.01	25±10	.002
Perfusion defected percentage (whole lung QDP) - %	6.5±5.0	19±19	.35	22±18	.10
Ventilation/perfusion match defect (V/Q defect) - %	0.5±0.8	3.9±4.7	.04	5.4±6.6	.002
Ventilation/perfusion match (V/Q match) - %	81±6.1	62±19	.006	60±20	.003

* Plus–minus values are means ±SD.

† Adjusted P Values tested with Kruskal-Wallis test and corrected Dunn's test for post-hoc comparisons between groups and given in comparison with healthy controls.

FIGURES

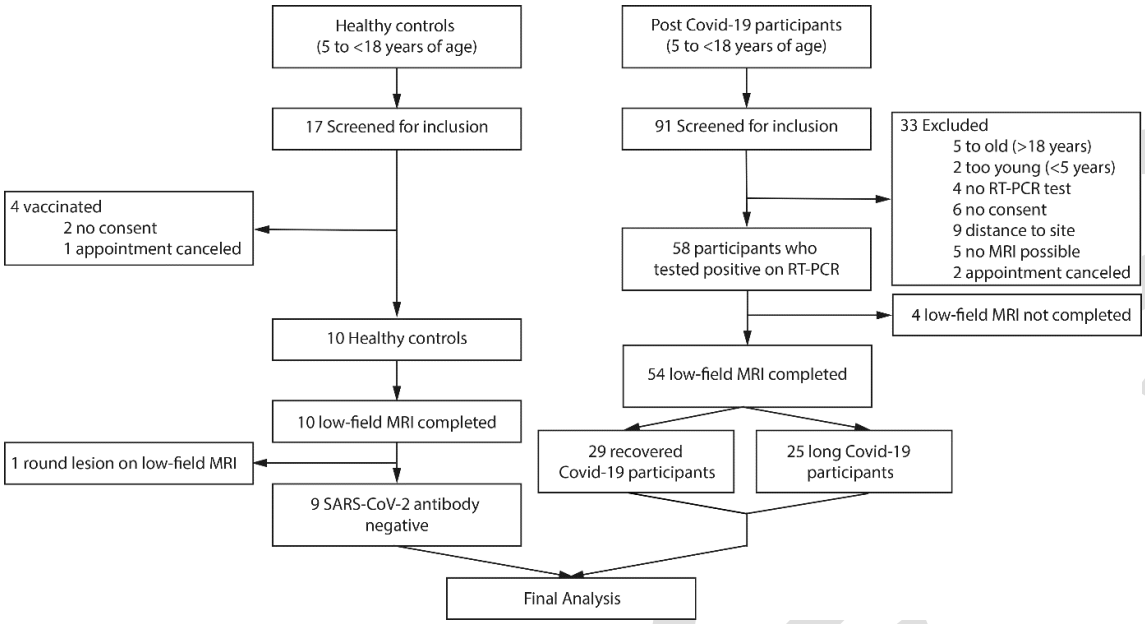

Figure 1. Flow chart of the study.

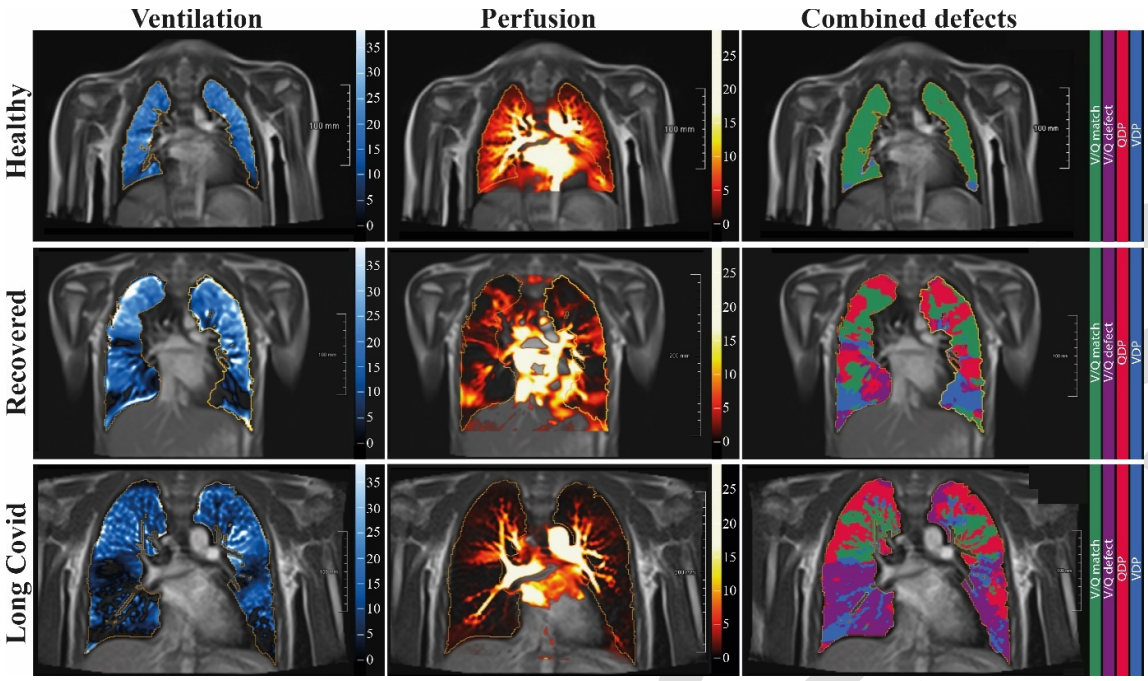

Figure 2. Free-breathing phase-resolved functional lung (PREFUL) low-field MRI at 0.55T with calculated parameters at an axial plane after automatic registration to a mid-expiration position and lung parenchyma segmentation**.** From left to right, representative color-coded images of functional show ventilation defects (VDP, blue), perfusion defects (QDP, red), ventilation/perfusion (V/Q match, green), ventilation/perfusion defects (V/Q defect, purple) in a healthy control (upper row, 7-year-old male), a participant recovered from COVID-19 (middle row, 10-year-old male) and a participant with long COVID (15-year-old male).

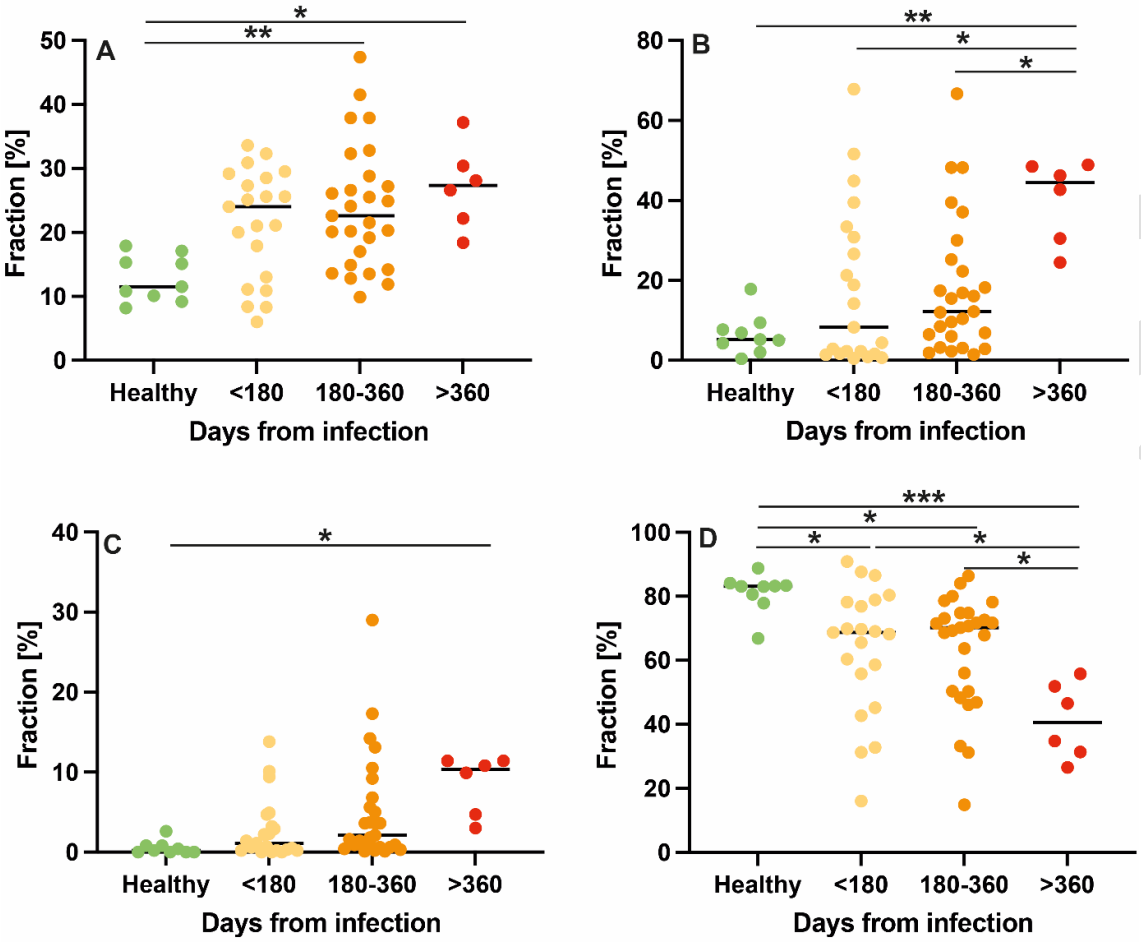

Figure 3. Comparison of low-field MRI parameters with respect to interval from first infection with dot plots for ventilation defects. The y-axis shows the fraction of defected or non-defected lung parenchyma on the automated measured axial plane. **(A)**, perfusion defects **(B)**, ventilation/perfusion match (no defects, **C**)) and ventilation/perfusion match (defect, **D**) in healthy controls, at less than 180 days, 180-360 days, and more than 360 days after SARS-CoV-2 infection.

Appendix E1

Supplement to: Heiss et al., Pulmonary dysfunction after pediatric COVID-19

This appendix has been provided by the authors to give readers additional information about the work.

Table of contents

Supplementary methods

Roche Elecsys® Anti-SARS-CoV-2 assay and Anti-SARS-CoV-2 -S assay

All blood samples were centrifuged and stored as serum at -15 degrees. For qualitative testing we used the electrochemiluminescence immunoassay (ECLIA) Elecsys Anti-SARS-Cov-2 assay according to the manufacturer's protocol. Briefly, it uses a recombinant protein representing the nucleocapsid (N) antigen in a double-antigen sandwich assay format, detecting antibody titer of all antibody isotypes (IgM, IgA, IgG). Test results exceeding 1.0 were interpreted as reactive, following the manufacturer's suggested Cut-off-index. Assay sensitivity was previously evaluated to have a sensitivity of 99.5% 14 days after the first positive RT-PCR results (95% CI: 97.0%-100%) and a specificity of 99.8% (95% CI: 99.69%-99.88%)".[43] All samples were further assessed on the same cobase 601 module with the Elecsys Anti-SARS-CoV-2-S immunoassay (ACOV2S). Anti-SARS-CoV-2 S is an immunoassay for the in vitro quantitative determination of antibodies to the SARS-CoV-2 spike (S) protein in human serum and plasma. It uses a recombinant protein representing the receptor binding domain of the spike protein enabling the identification of highly affine SARS-CoV-2 IgM and IgG antibodies using a double antigen sandwich immunoassay. All samples were processed according to the manufacturer's instructions. Test results exceeding 0.8U/ml were considered reactive, following the manufacturer's suggested cut-off-index. Values between 0.40–250 U/mL represent the linear range. Samples above 250 U/mL were automatically diluted into the linear range of the assay (realized dilutions in this study: 1:10 or 1:100) with Diluent Universal (Roche Diagnostics). The analyzer automatically multiplies diluted results with the dilution factor, which in the applied setting enabled an upper limit of quantification of 25000 U/mL for these analyses. The assay demonstrated a sensitivity of 98.9% (95% CI: 98.1%-99.3%) 14 days after the first positive RT-PCR result and a specificity of 99.96% (95% CI: 99.91%-100%).[44]

The assigned U/mL are equivalent to Binding Antibody Units (BAU)/mL as defined by the first World Health Organization (WHO) International Standard for anti-SARS-CoV-2 immunoglobulin (NIBSC code 20/136). The reported results in U/mL can be directly compared with other studies or results in BAU/mL. No conversion of units is required.

Serum Interleukin 6 (IL-6) was measured by electrochemiluminescence immunoassay (Elecsys IL-6, Cobas e601). C-reactive protein (CrP) was measured using a standard immunoturbidometric assay on the Cobas c501 system (Roche Diagnostics).
Complete blood counts were performed using Sysmex XE-2100 (Sysmex, Kobe, Japan) analyzers.

Supplementary Tables

Table E1 – **Pre-existing conditions in participants**

Condition	Healthy (n=9)	Recovered (n=29)	Long Covid (n=25)
Allergy/Hypersenisitvity/Atopic			
• Grasses, willow, poplars, house dust, rye	0 (0)	0 (0)	1 (4)
• Histamin	0 (0)	0 (0)	1 (4)
• Wasp Venom	0 (0)	0 (0)	1 (4)
• Atopic dermatitis	0 (0)	0 (0)	1 (4)
• Mastozytosis	0 (0)	1 (3)	0 (0)
Cardiopulmonary			
• Corrected venticel septum defect	0 (0)	1 (3)	0 (0)
• Sinus venosus	0 (0)	1 (3)	0 (0)
• Bronchial asthma	0 (0)	0 (0)	2 (8)
Metabolic/Endocrinology			
• Hypercholesterinemia	0 (0)	1 (3)	0 (0)
• Hypothyreosis	0 (0)	0 (0)	1 (4)
Celias diaseasee	0 (0)	0 (0)	1 (4)
Von Willebrand's disease	1 (11)	0 (0)	0 (0)
Slight mucular hypotonia	1 (11)	0 (0)	0 (0)
Funnel chest	0 (0)	0 (0)	1 (4)
Attention Deficit Hyperactivity Disorder	0 (0)	1 (3)	1 (4)
Total	**2 (22)**	**5 (17)**	**10 (40)**

Note—Data in parentheses are percentages.

Table E2 – Acute and post-acute symptoms of the study sample

Characteristic	Healthy control (N=9)	Post COVID-19 (N=54)
Acute Symptoms during SARS-CoV-2 infection – no. (%)		
Headache	N/A	29 (54)
Rhinitis	N/A	29 (54)
Sore throat	N/A	23 (43)
Cough	N/A	25 (46)
Shortness of breath	N/A	8 (15)
Pneumonia	N/A	0 (0)
Fever	N/A	22 (41)
Anosmia	N/A	13 (24)
Ageusia	N/A	17 (31)
Fatigue	N/A	10 (19)
Diarrhea	N/A	1 (2)
Limb pain	N/A	5 (9)
Post-acute Symptoms after SARS-CoV-2 infection – no. (%)		
Headache	N/A	5 (9)
Dyspnea	N/A	15 (28)
Pneumonia	N/A	1 (2)
Fever	N/A	0 (0)
Anosmia	N/A	4 (7)
Ageusia	N/A	1 (2)
Fatigue	N/A	4 (7)
Impaired attention	N/A	6 (11)
Limb pain	N/A	1 (2)
Shortness of breath	N/A	16 (30)

Note—Data in parentheses are percentages.

Table E3 – Quantitative measurements of free breathing phase-resolved function lung MRI*

Parameter	Healthy control (N=9)	Recovered (N=29)	P Value†	Long COVID (N=25)	P Value†
Mean FVL Correlation	0.9±0.03	0.9±0.06	.17	0.9±0.10	.25
$VDP_{Exclusive}$ - %	12±3.4	18±6.8	.04	19±8.2	.03
$VDP_{FVL,Exclusive}$ - %	9.2±3.9	14±7.5	.26	15±9.4	.24
VDP_{FVL} - %	9.8±4.1	17±9.5	.12	20±13	.06
$QDP_{Exclusive}$ - %	6.0±4.3	15±15	.58	17±14	.15
$VQM_{Defect, FVL}$ - %	0.6±0.8	3.4±4.2	.29	5.1±7.9	.04
$VQM_{Non-defect, FVL}$ - %	85±7.4	67±21	.06	62±22	.02

* Plus–minus values are means ±SD.

† Adjusted P Values tested with Kruskal-Wallis test and corrected Dunn's test for post-hoc comparisons between groups and given in comparison with healthy controls.

Supplementary Figures

Figure E1 – Image acquired in an eight-year-old male participant recovered from COVID-19. Unenhanced axial Turbo-Spin-Echo (TSE) sequence with BLADE (periodically rotated overlapping parallel lines with enhanced reconstruction) readout and respiration-gating. Arrows indicate linear atelectasis. Asterisk marks a partial volume effect caused by adjacent liver parenchyma.

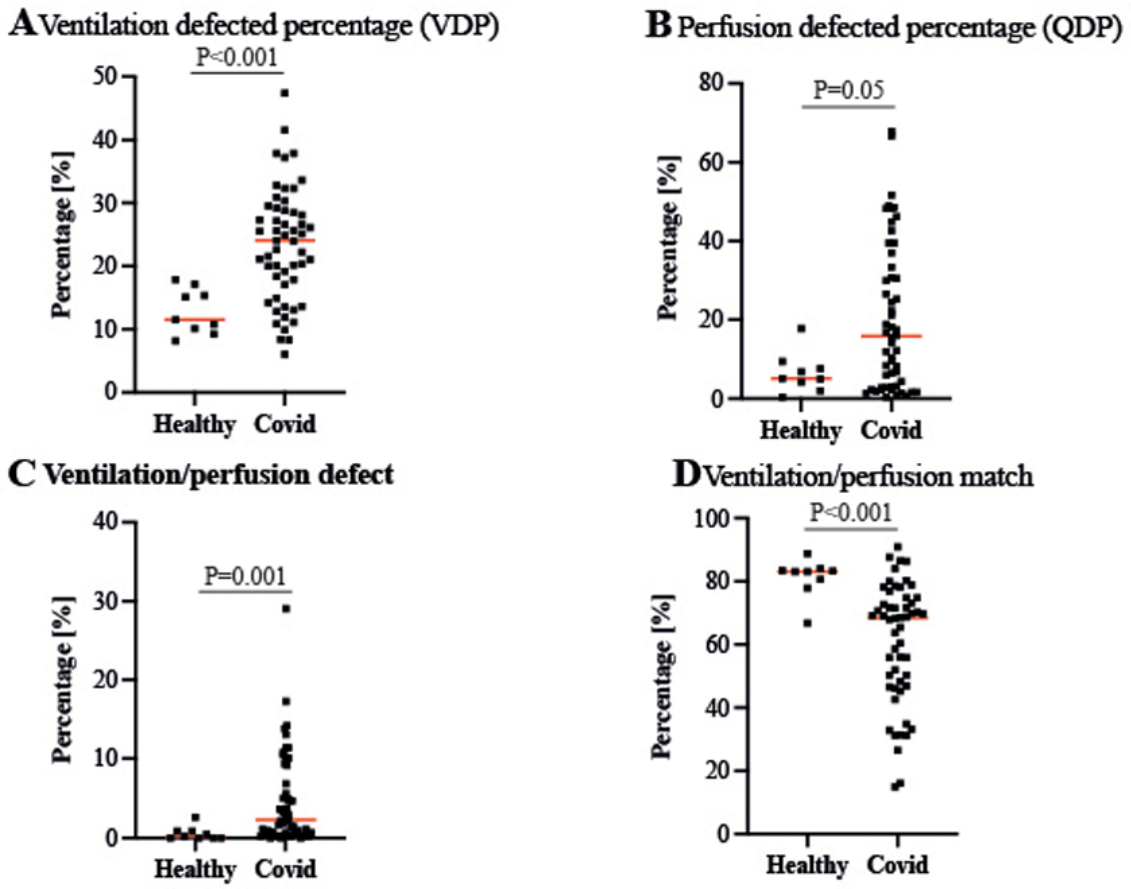

Figure E2 – Low-field MRI measurements in participants with post-acute COVID-19 (n=54) vs. healthy controls (n=9). All tests were performed with nonparametric Mann-Whitney test.

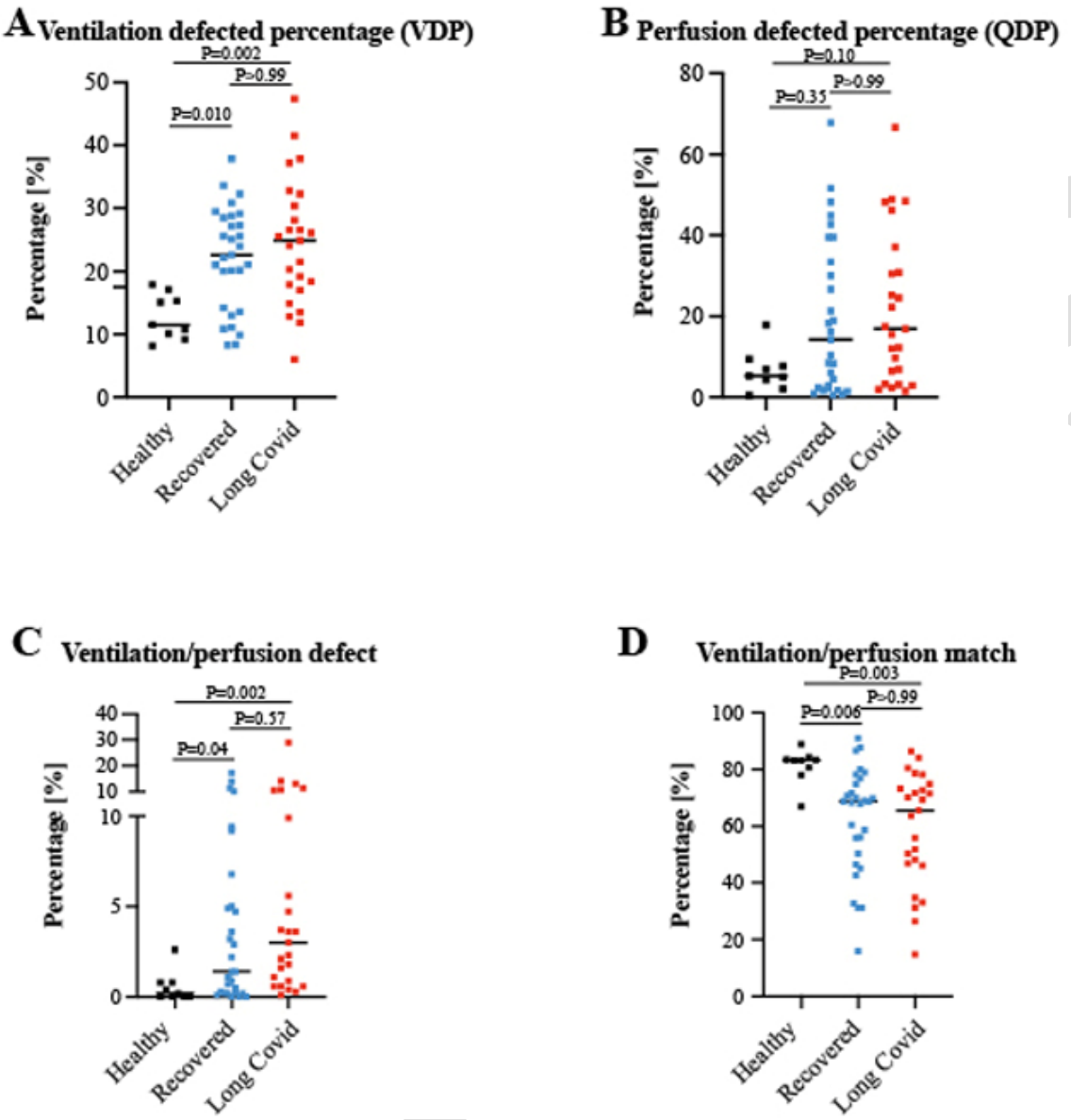

Figure E3 – Low-field MRI measurements in healthy controls (n=9), participants recovered from COVID-19, (n=29) and participants with long COVID (n=25).
P values were tested with Kruskal-Wallis test and corrected Dunn's test for post-hoc comparisons between groups in comparison with healthy controls. Adjusted p values are reported.

A Healthy control, 7 years, male

B Recovered Covid-19 patient, 10 years, male

C Long Covid patient, 15 years, male

Figure E4 – Images acquired in a healthy control (male, 7 years), participant recovered from COVID-19 (male, 10 years) and a participant with long COVID (male, 15 years). Unenhanced axial Turbo-Spin-Echo (TSE) sequence with BLADE (periodically rotated overlapping parallel lines with enhanced reconstruction) readout and respiration-gating.

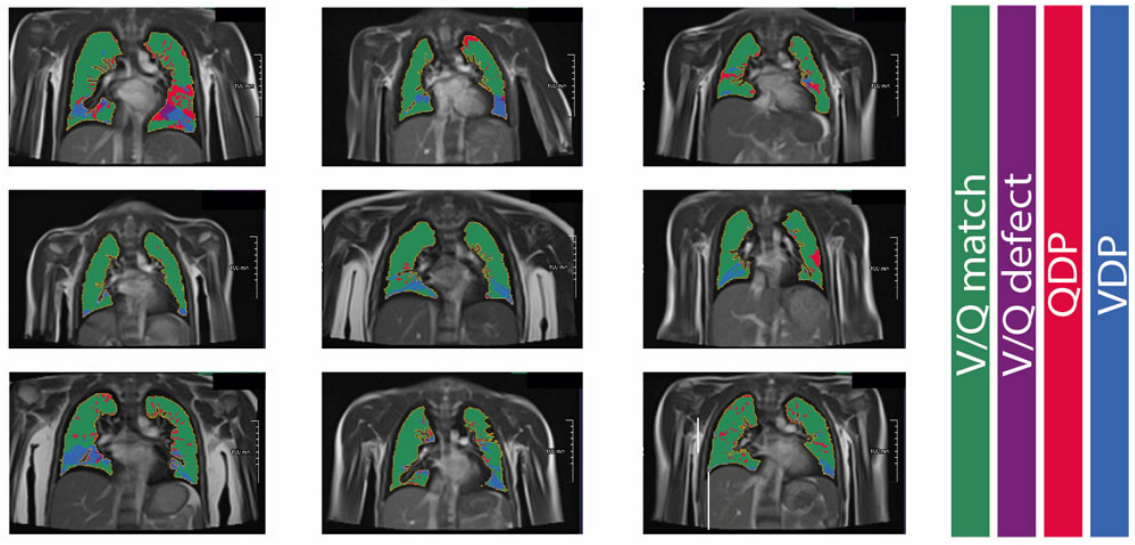

Figure E5 – Free-breathing phase-resolved functional lung (PREFUL) low-field MRI with calculated parameters at an axial plane after automatic registration to a mid-expiration position and lung parenchyma segmentation in healthy controls.
V/Q match = ventilation/perfusion match (green); V/Q defect = combined ventilation/perfusion defect (purple); QDP = perfusion defect percentage (red); VDP = ventilation defect percentage (blue).

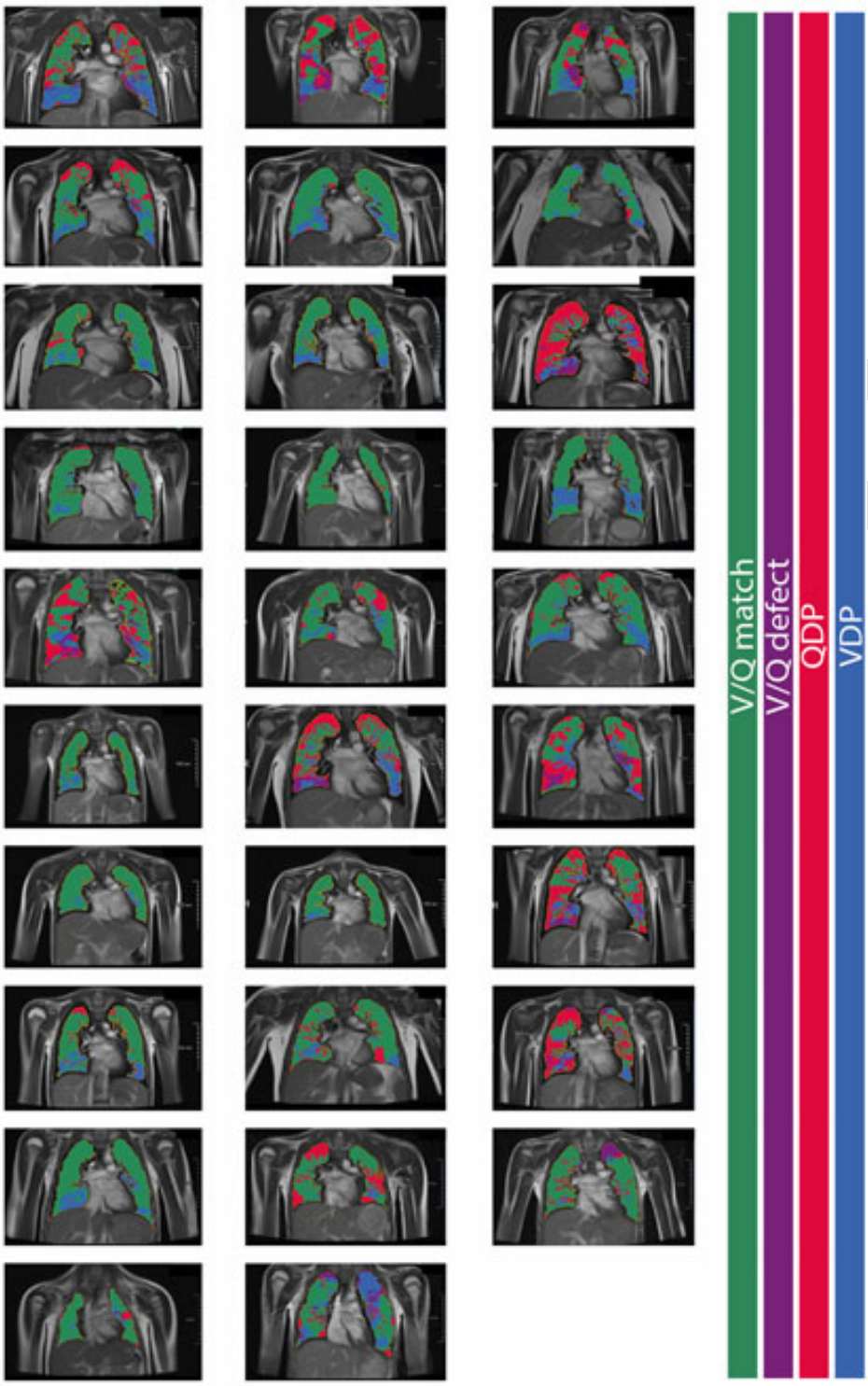

Figure E6 – Free-breathing phase-resolved functional lung (PREFUL) low-field MRI with calculated parameters at an axial plane after automatic registration to a mid-expiration position and lung parenchyma segmentation in participants recovered from COVID-19.
V/Q match = ventilation/perfusion match (green); V/Q defect = combined ventilation/perfusion defect (purple); QDP = perfusion defect percentage (red); VDP = ventilation defect percentage (blue).

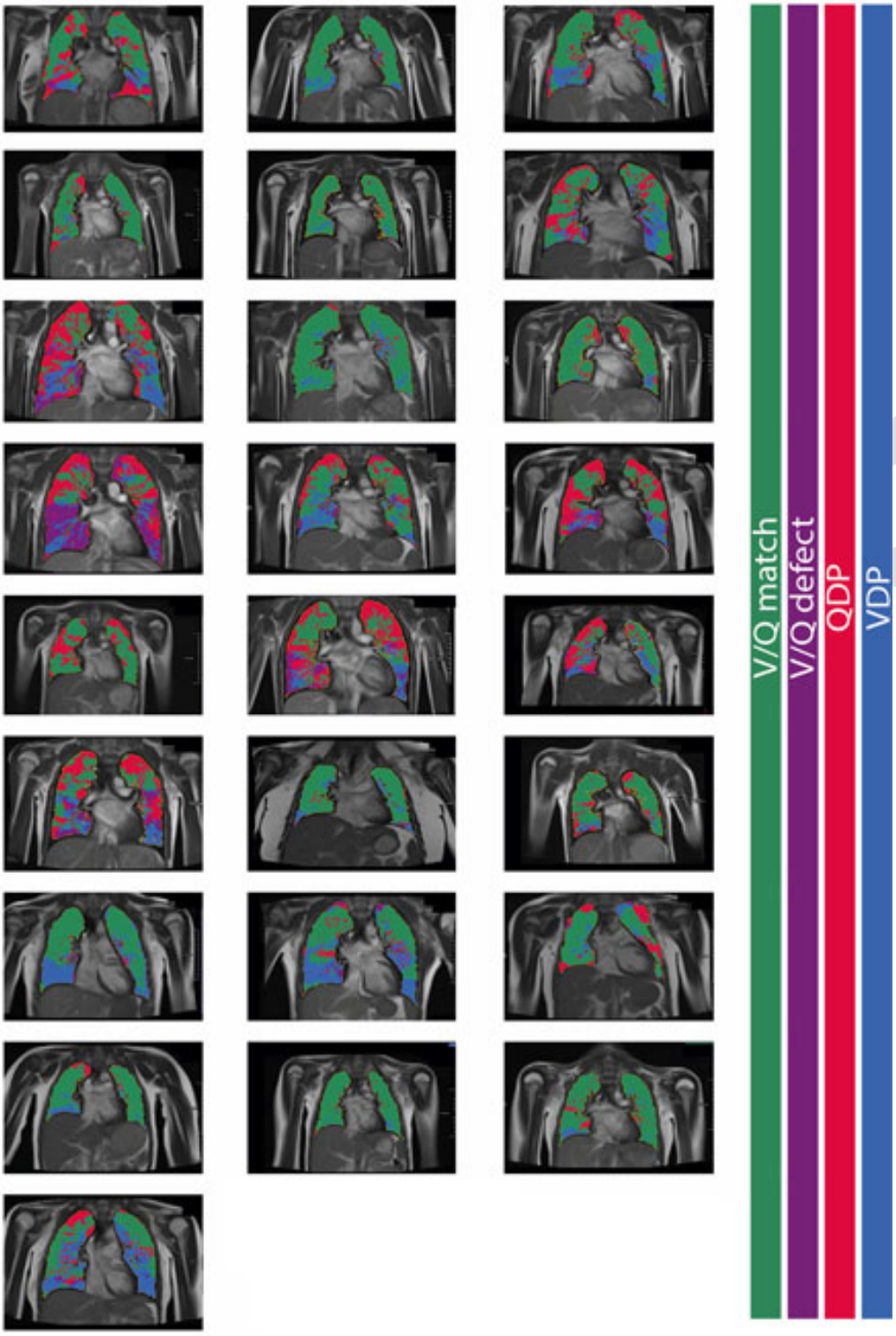

Figure E7 – Free-breathing phase-resolved functional lung (PREFUL) low-field MRI with calculated parameters at an axial plane after automatic registration to a mid-expiration position and lung parenchyma segmentation in participants with long COVID.
V/Q match = ventilation/perfusion match (green); V/Q defect = combined ventilation/perfusion defect (purple); QDP = perfusion defect percentage (red); VDP = ventilation defect percentage (blue).

Supplemental References

42 Muench, P. *et al.* Development and Validation of the Elecsys Anti-SARS-CoV-2 Immunoassay as a Highly Specific Tool for Determining Past Exposure to SARS-CoV-2. *J Clin Microbiol* **58**, doi:10.1128/JCM.01694-20 (2020).

43 *Fact sheet, ElecsysT Anti-SARS-CoV-2 S*, <https://assets.cwp.roche.com/f/94122/x/379ebe6732/factsheet-elecsys-anti-sars-cov-2-s_v1.pdf>